

# Energy-efficiency of all-optical transport through time-driven switching

F. Musumeci<sup>1</sup> M. Tornatore<sup>1</sup> G. Fontana<sup>2</sup> M. Riunno<sup>3</sup> S. Bregni<sup>1</sup> A. Pattavina<sup>1</sup>

<sup>1</sup>Department of Electronic and Information, Politecnico di Milano, via Ponzio 34/5, 20133 Milano, Italy

<sup>2</sup>Faculty of Science, University of Trento, 38050 Povo, TN, Italy

<sup>3</sup>Fastweb S.p.A., via Caracciolo 51, 20155 Milano, Italy

E-mail: [fmusumeci@elet.polimi.it](mailto:fmusumeci@elet.polimi.it)

**Abstract:** Decreasing the Internet power consumption is a challenging issue. Optical transport networks employing the wavelength division multiplexing (WDM) technique have been identified as energy efficient solutions to face this issue, considering the expected high increase of Internet traffic. The authors study the energy efficiency of a recently-proposed switching technique for transport networks, the time-driven-switching (TDS), in which time-coordination of network elements is exploited to achieve ‘sub-lambda’ granularity in optical signal switching directly in the optical domain. In order to achieve the fast switching time required by TDS, semi-conductor optical amplifier-based optical switches are exploited. The authors discuss the properties, in terms of the energy efficiency, of a TDS transport network, focusing on the energy requirements of the TDS optical switches. The authors provide a qualitative description of the main contributors to energy consumption in a TDS network. The authors then develop an integer linear programming formulation, in which the physical impairments impact over optical signals is also considered. Power consumption over realistic case study networks for the TDS case is compared to the power consumption for the classical IP over WDM architecture, and in some cases TDS is demonstrated to save more than 55% of power consumption with respect to competing architectures.

## 1 Introduction

The predicted growth of the future Internet traffic and, in general, of the number of devices connected to the network, will lead to a sheer increase of the energy consumption of telecommunication networks in the next years. The most widely-used solution adopted to achieve substantial savings in telecommunication networks cost consists in deploying optical technologies that exploit the wavelength division multiplexing (WDM) technique. As a further advantage, this technique also allows to efficiently face the energy consumption problem arising with the envisioned traffic increase. WDM networks are capable to route wavelength channels (i.e. lightpaths), each carrying one (or more) electronic tributary signal(s) from source to destination nodes through a series of optical fibre links and, in most of cases, with no need to perform data processing. By doing so, significant reduction in the number of optical/electronic/optical (OEO) signal conversions, that require high power consumption because of the opto-electronic devices needed, and in the amount of electronic processing operations can be obtained.

Many recent works have discussed the energy efficiency of the transport layer of optical networks. The approach used in [1] evaluates the power consumption in an optical network by considering the power consumption of an individual lightpath and thus obtaining the overall consumption as a function of the number of lightpaths. In [2] the concept of

lightpath-bypass is exploited to design an IP-over-WDM network that minimises power consumption by reducing the number of needed IP router ports. Moreover, in [3] a comprehensive comparison, from the energy consumption point of view is performed by the authors for different transport network architectures.

In this paper we study the energy consumption of a recently proposed switching technique, known as time-driven-switching (TDS), that exploits the time coordination of network elements in order to obtain the capability of switching fractions of wavelengths (lambdas) and perform aggregation (grooming) and separation (degrooming) of traffic flows directly in the optical domain [4]. This objective is achieved thanks to the semi-conductor optical amplifier (SOA) technology, exploited as it enables fast switching times (in the order of hundreds of picoseconds [5]) as required in TDS networks [the TDS efficiency-loss (e.g. because of guard bands needed) can still be considered acceptable for 40 or 100 Gbit/s data rates]. Moreover, we provide a qualitative assessment of the different power consumption contributions of such SOA-based optical switches. Then we compare the energy consumption of a TDS transport architecture with the consumption of classical IP-over-WDM (IPoWDM) transport architectures by developing an integer linear programming (ILP) formulation for the design of energy-minimised optical transport networks. We will show that TDS provides up to more than 55% of power saving if compared to the IPoWDM architecture.

The paper is organised as follows: in Section 2 we overview the main concepts of a TDS network and describe the TDS node architecture. In Section 3 we first identify the network elements that contribute to the overall energy consumption of the TDS transport network, then we investigate the issue of the energy consumption within an SOA-based switch and study the energy trade-offs between different SOA-switch architectures. Section 4 defines, through an ILP formulation, the problem of energy consumption minimisation in a TDS network, whereas results of the comparison between TDS and the classical IPoWDM network architectures are presented in Section 5. Finally, the paper conclusion is drawn in Section 6, where we also address possible future works.

## 2 Time-driven-switched networks

The application of TDS in optical transport networks relies on the implementation of the pipeline forwarding technique [4], by exploiting the time-coordination of all network elements. A global time reference, that is today ‘freely available’ from a variety of sources on earth and in space (such as GPS and Galileo), is used so that a basic time period, called time frame (TF), can be identified. TFs are grouped into time cycles (TCs) and TCs are further grouped into super cycles, each of them lasting for one universal coordinated time (UTC) second, as shown in Fig. 1a, where we assume that a UTC second is composed by a set of 100 TCs, each consisting of 1000 TFs of duration  $T_f$ . TFs are partially or totally reserved for each flow during a resource-reservation

procedure; the TC sets the periodicity of the reservation. This results in a periodic schedule, repeated every TC, for packets to be switched and forwarded, which is called synchronous virtual pipe (SVP), or fractional  $\lambda$  Pipe in the context of optical networks. Fig. 1b shows how an SVP is switched and forwarded along three optical switches A, B and C: the propagation delay among the switches is expressed in terms of multiples of TFs. Each SVP transports data of one protocol, such as IP, multi protocol label switching (MPLS) packets or asynchronous transfer mode (ATM) cells. However, SVPs transported over the same wavelength on a certain link may carry data of different protocols, as TDS is ‘transparent’ to modulation and bit-rate since data is always maintained in the optical domain. The content of each TF is switched according to its position within the TC. Therefore label or header processing is not necessary in each intermediate node. Note that TDS with pipeline forwarding introduces an additional constraint to the establishment of an SVP: the so-called ‘TF continuity’ along the whole path, that is, a packet reaching a network node needs to be immediately switched towards the next node, without being buffered (i.e. the switch is performing ‘immediate forwarding’).

### 2.1 TDS node architecture

We now define the architecture of a TDS node and the devices used therein. In Fig. 2a the model of a TDS node is shown. An upper layer made up of IP routers is placed over an optical layer consisting of optical cross connects (OXC)

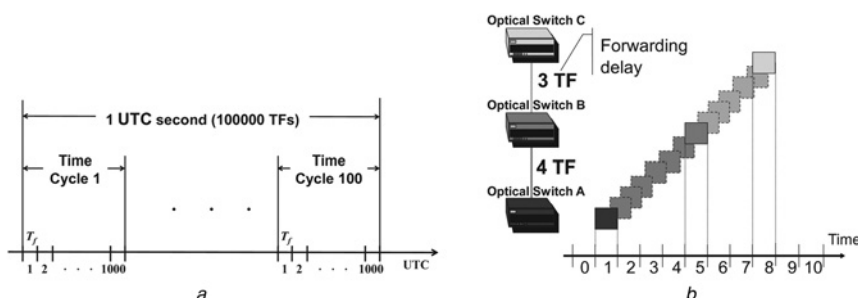


Fig. 1 TDS features

- a Common time-reference structure
- b Switching of a SVP

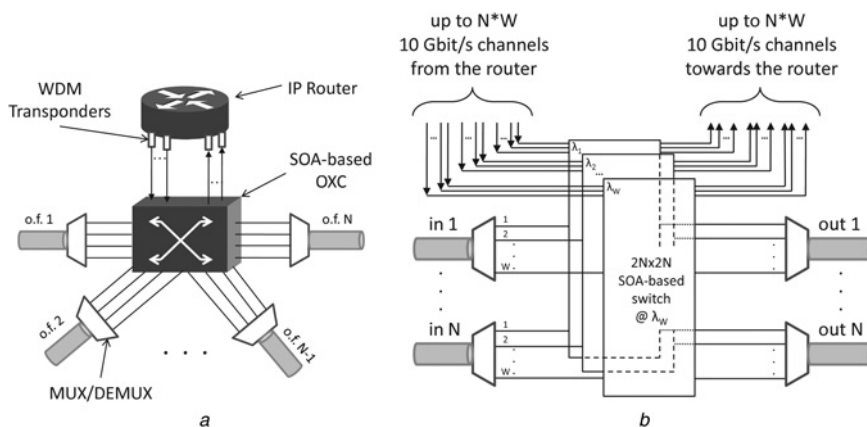


Fig. 2 Model of a TDS node

- a TDS node architecture with incoming/outgoing optical fibre (o.f.) links
- b Structure of the SOA-based OXC within the node

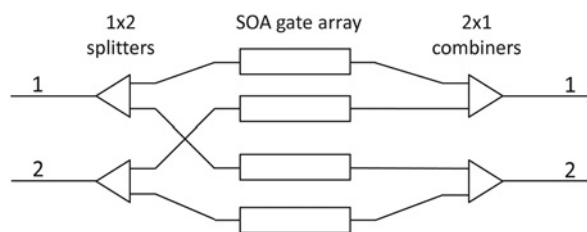


Fig. 3  $2 \times 2$  SOA-based switch architecture

and optical fibre links, connected to the OXCs through multi/demultiplexing stages. The interconnection between the IP routers and the OXCs is usually performed through WDM transponders, intended as receiving/transmitting devices (i.e. router ports) that provide the OE and EO signal conversion. In order to implement TDS in the optical domain [note that the principles of TDS can be also exploited in the electronic domain, although it requires OE and EO conversion operations, which are not needed when switching is performed in the optical domain], optical switches must support a very fast reconfiguration time, that matches the very short duration of a TF (i.e. the smallest granularity to be switched in TDS, which is on the order of  $10 \mu\text{s}$ , according to Fig. 1a). Switching fabrics based on SOAs can provide this very fast switching time (down to the order of hundreds of picoseconds), therefore SOA-based OXCs will be considered in the following. The structure of such OXCs is shown in Fig. 2b, where we assume that the switching operations are performed through a multiple-plane switching architecture, where each plane operates over demultiplexed signals with a certain wavelength. A generic node is reached by  $N$  (bidirectional) WDM links, each carrying up to  $W$  different wavelength channels. When an optical signal arrives at the input of the node through the optical fibre link, the different  $\lambda$ s are demultiplexed and each  $\lambda$  is sent towards its appropriate SOA-based switch plane, that provides for switching of signals coming from (going to) a specific input (output) link. Up to  $N$  additional inlets/outlets per plane need to be taken into account, since an IP router can be source/destination for up to  $N$  (one for each input/output link) SVPs over the  $W$  wavelengths. Therefore we consider  $2N \times 2N$  SOA-based switches, that can be obtained using elementary  $2 \times 2$  switches implemented through a broadcast-and-select structure, exploiting SOAs as well as  $1 \times 2$  splitters and  $2 \times 1$  combiners, as depicted in Fig. 3.

The elementary  $2 \times 2$  switches are then replicated in Banyan structures [6] in order to obtain strict-sense non-blocking  $M \times M$  switches. Therefore each signal switched by such an  $M \times M$  device, traverses a number of SOAs equal to  $\log_2 M$ . However, as we will see in the following, this approach is not the most efficient from the energy consumption point of view, since other structures can be employed to obtain devices requiring a lower amount of energy. From an economic point of view, the technology employed in TDS networks still needs to be improved, in order to be appealing for a large scale introduction to market. Although GPS cards (combined with rubidium or cesium clocks to obtain time synchronisation among all nodes in the network) are available from multiple vendors and relatively cheap (\$100–200), SOA-switch technology is nowadays far more expensive than currently employed optical switches, such as arrayed waveguide gratings, micro-electro-mechanical systems (MEMS), micro-ring resonators (MRRs) etc. However, designing a network by

taking into account both CAPital/OPERational EXPENDITURE (CAPEX and OPEX) suggests that TDS networks could soon represent a practical solution for optical transport networks.

### 3 Power consumption contribution within a TDS transport network

The energy-consumption of TDS transport networks will be evaluated by considering an ILP optimisation problem which, given a transport network topology and a fixed set of required connections between each node pair, aims at minimising the total power consumed by the network. Results will be compared with those of a classical IPoWDM network architecture, identified as transparent IP with bypass and grooming (T. IP-BG) in [3], in which traffic grooming is performed into the electronic domain by IP routers.

Different contributions should be considered when dealing with transport networks power consumption, such as:

- electronic traffic processing performed at the IP layer by routers;
- control operations (e.g. signaling, clock recovery etc.);
- transmitting/receiving devices (i.e. WDM transponders) and short-reach interfaces;
- optical and/or electronic switching devices;
- optical amplifiers (usually erbium doped fibre amplifiers (EDFAs)).

In the following, we consider only those contributions that depends on the specific adopted transport architecture (i.e. those contributions, who are different in TDS against IPoWDM). For instance, in a first approximation, the contribution because of EDFAs can be neglected, since they are supposed to be pre-deployed independently of the switching architecture, therefore their number (and thus, their overall contribution) does not vary with the considered architecture. The same observation can be made for the control operations. In fact, the consumption of local schedulers, usually implemented through field programmable gate arrays (FPGAs), can be a limiting factor for TDS networks, as a higher number of switch-control operations are required if compared with classical IPoWDM networks. However, FPGAs technology is improving in these years so that their energy requirements can be neglected as each consumes less than 100 mW (see [7, 8] for FPGA power estimation). Moreover, the timing-information distribution among TDS switches is needed and it is accomplished through GPS cards, placed in each node to locally provide the clock for switch configuration. Therefore in a first approximation, the GPS cards consumption represents the only additional power contribution with respect to the IPoWDM case (where global schedulers still need to control optical switches all over the network). Nonetheless, GPS cards are nowadays very efficient from the energy point of view as each is estimated to require about 200–300 mW [9]. Furthermore, the energy contribution because of electronic processing of traffic is only considered within intermediate nodes, since electronic traffic processing in source/destination nodes requires the same consumption in both the TDS and IPoWDM cases. Therefore in the following we only consider three power contributions, that still represent the main power-requiring factors, that is:



1. Electronic processing: in intermediate nodes: it is considered whenever traffic grooming (and switching) in the electronic domain or signal regeneration operations need to be performed. A high-power consumption is needed in these cases, estimated to be on the order of 14.5 W per Gbit/s of processed traffic [10];
2. WDM transponders: transmitting and receiving devices are used in source and in destination nodes, but they are also employed when OE and EO conversions are performed in intermediate nodes. Each of these devices converts 10 Gbit/s signals from (into) a specific wavelength and the power consumed by such a device is assumed to be 34.5 W [10];
3. Optical switching: we consider two different kinds of optical switches: MEMS-based OXCs, used in the IPoWDM architecture [although MEMS switches suffer from a slow tuning speed (which makes them impractical to be used in high-speed optical networks), we consider such devices as we perform a static design of the network, hence we do not need to re-configure the switches in our study], consume 1.5 W each time a 10 Gbit/s wavelength is switched [11]. For the TDS architecture SOA-based OXCs are considered and their consumption is estimated to be on the order of 500 mW, as one SOA can be used in such devices to switch a wavelength channel (see Section 3.1 and 3.2).

In the following, the described contributions will be indicated as  $\Pi_e$ ,  $\Pi_i$  and  $\Pi_o$ , respectively.

### 3.1 On the power consumption of an SOA-based optical switch

SOA technology is well established and future developments are only expected to impact large scale integration of the devices and let overall power considerations only marginally affected except for a global technology factor. Considering switching architectures built around passive optical shuffle networks (i.e. multistage networks where passive splitters and combiners are used to connect each input port with each output port) [6] and SOA gating and amplification, it is possible to define the range of switch sizes that are compatible with the SOA technology in order to estimate the power consumption. As optical shuffle networks are composed by optical fibre couplers that introduce losses proportional to the number of input/output fibres, SOAs must provide both the switching function and the loss recovery function in order to achieve an acceptable BER (i.e. compliant to the standard of the transport layer in use). Let us calculate the conventional gain of a possible SOA-based passive shuffle architecture for increasing number of inputs/outputs  $M$  in non-blocking switches. The gain of the SOA is assumed to be 25 dB, a figure that may not improve much in the future, so the input-to-output gain as a function of  $M$  is given by:

$$\text{Input to output gain (dB)} = 25 \text{ dB} + 20 \log_{10}(1/M) \text{ dB} \quad (1)$$

It follows that, even under ideal conditions, it is not possible to build a non-blocking switch larger than  $16 \times 16$  with passive shuffle networks. In fact an ideal 16 fibre coupler will split input power by 16, with a power reduction of  $-12$  dB on each output fibre. Considering both input and output shuffling networks, the total power reduction is  $-24$  dB, with total overall gain of the switch of only 1 dB under ideal conditions. Smaller switches with zero overall

gain will require less gain from the SOAs, and this can positively impact on power consumption. In fact, generally the gain of a typical SOA is still above 20 dB with operating current down to 40% of nominal current [12]. Below 40% of nominal current the optical gain drops sharply, reaching 0 dB at about 20% of nominal current.

Our group has already implemented testbed versions of SOA switches for a TDS network [13], and we have collected useful information to assess the energy consumption of these switches. SOAs employed in our  $2 \times 2$  switch design (see Fig. 3) can be operated at 100 mA in the ON state and 0 mA in the OFF state with an overall switch gain of few dB suitable for driving short fibres [the SOA operating current must be increased to 300 mA if the switch is intended to drive long (tens of kilometres) fibres without additional amplification. However, in our model, each switch is equipped with pre-amplifiers and thus their consumption is neglected in the following optimisation problem, so no additional amplification from the SOAs is required]. To estimate the power required by an SOA switch it is necessary to assess the voltage and the duty-cycle of the individual SOAs of the switch. According to the manufacturer the voltage is about 1.3 V and it slightly depends on the operating current. For non-blocking switches with passive shuffle networks the maximum power requirement is proportional to the number of outputs, that is, 130 mW per output. Beyond  $16 \times 16$ , non-blocking switches are possible with active shuffle networks with additional power required by intermediate amplifiers. If the switch is organised in a Banyan network, the power requirement is the power required by a single SOA times  $M \log_2 M$ . In fact all SOAs along a path must be ON. The calculation does not take into account the energy efficiency of the driving electronics and temperature regulation. Highly optimised driving electronics for commercial applications will increase the overall power requirements by an additional 20%, on the other hand in laboratory prototypes the energy efficiency of SOA drivers could be much lower because unconditional SOA integrity and parameter tuning capability requirements dominate over efficiency and cost. Laboratory drivers based on a controllable linear constant current source powering the SOA and a high speed shunt network connected in parallel to divert the current from the SOA, provide simpler but less energy efficient solutions. If the circuitry is powered by a 5 V power supply, it constantly draws the operating SOA current, therefore the power requirement is 500 mW per SOA. From the above considerations it emerges that with efficient driving electronics non-blocking switches must be preferred for switch size up to  $16 \times 16$ . Energy efficiency and non-blocking architecture do indeed require a large number of SOAs ( $M^2$ ) while only  $M$  are simultaneously powered. Banyan switches are simpler and cheaper, requiring less SOAs, but they are susceptible to blocking and require more power by a factor of  $\log_2 M$ . Therefore in the following (see Section 3.2) non-blocking switches will be considered since they match the energy efficiency issue we want to address in this paper.

Noise limitations must also be considered. SOAs are affected by amplified spontaneous emission (ASE) noise, gain modulation and, consequently, crosstalk among wavelengths. Remedies to signal degradation because of these phenomena are well known. Forward and backward ASE noise can affect the gain of each SOA and subtracts power to the useful signal in multistage SOA switches [14]. Narrowband optical filters and circulators can be introduced

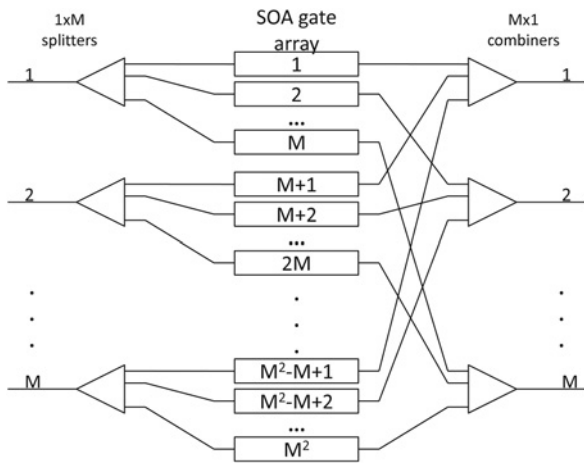


Fig. 4 Extended  $M \times M$  SOA-based switch architecture

in the switch to block out of band noise and backward ASE propagation, respectively [15]. The fundamentally analogue nature of the system we are discussing will require the adoption of optical signal regenerators and clock and data recovery (CDR) to minimise the overall error rate. Regarding amplitude noise, after wavelength extraction from a WDM fibre, saturated SOAs can perform noise reduction [16]. If required, CDR can be easily performed electronically at the switch boundary, and will require wavelength extraction and processing. Cascaded SOA have been demonstrated up to 11 stages with simulations up to 20 and more.

### 3.2 Energy-efficiency for alternative SOA-switch architectures

In the previous section we have assumed an SOA-based OXC architecture consisting of  $W$  planes. Each of these planes is dedicated to a specific wavelength among the  $W$  carried by optical fibre links and consists of an  $M \times M$  switch (for sake of simplicity we assume  $M$  as an even number, that is,  $M = 2N$ ) operating at a specific wavelength.

Many structures can be employed to realise the  $W$  planes. The structure of Fig. 3 can be extended using, for example,  $1 \times M$  splitters and  $M \times 1$  combiners and an SOA gate array with  $M^2$  SOAs, as in Fig. 4, where we show the ‘extended’  $M \times M$  architecture. The number of SOAs required by this architecture (which increases as  $M^2$ ) is high if compared to a Banyan structure, where the number of SOAs increases as  $M \log_2 M$ . However, this approach is more energy-efficient since only one SOA is traversed by each switched signal. Thus in the following we consider the SOA-switch architecture as in Fig. 4, where power in the order of 500 mW is required to switch one wavelength.

## 4 Power-consumption minimisation problem

In this section, we formally define and provide an ILP formulation for the power-consumption minimisation problem in a TDS network, which will be then compared with a classical IPoWDM architecture in terms of power consumption. Given a double-layer network consisting of IP routers placed over an optical WDM layer (OXCs connected by optical fibre links) and a set of traffic demands among the nodes, we aim at minimising the power consumption of the transport network while satisfying three main sets of constraints: (i) all the requests must be routed

in the network, (ii) each fibre carries a limited number of wavelengths and (iii) each signal is maintained at a certain wavelength as long as it is not converted into the electronic domain.

The inputs of the problem are the following:

- $G = (N, A)$  is the physical topology of the network, composed by a set  $N$  of nodes, each corresponding to an IP router connected to an OXC and a set  $A$  of bidirectional arcs, corresponding to fibre links, connecting the nodes; we indicate as  $N_m$  the set of all nodes adjacent to node  $m$ , that is,  $N_m = \{n \in N | (m, n) \in A\}$ ;
- $R$  is the set of traffic requests, with source and destination nodes of the  $r$ th request,  $r \in R$ , indicated as  $s(r)$  and  $d(r)$ , respectively, and the corresponding required bandwidth indicated as  $t_r$ ;
- $L$  is the set of wavelengths carried by each fibre ( $|L| = W$ );  $C$  is the capacity, in Gbit/s, of each wavelength;
- $\Pi_e$ ,  $\Pi_t$  and  $\Pi_o$  are the power contributions described in Section 3.

### 4.1 ILP formulation

#### 4.1.1 Variables

$X_{ij}^r$  equal to 1 iff request  $r \in R$  is served by the logical link between the nodes  $i, j \in N | i \neq j$  (binary).

$Y_{ijl}^r$  amount of traffic of the request  $r \in R$  served by the logical link between the nodes  $i, j \in N | i \neq j$  over wavelength  $l \in L$  (integer).

$V_{ijl}$  total amount of traffic between the nodes  $i, j \in N | i \neq j$  over wavelength  $l \in L$  (integer).

$P_{mnl}^{ij}$  amount of traffic over wavelength  $l \in L$  between the nodes  $i, j \in N | i \neq j$  traversing the physical link  $(m, n) \in A$  (integer).  $T_{mnl}$  equal to 1 iff in node  $m \in N$  a transmitting transponder on wavelength  $l \in L$  is used to transmit a signal towards node  $n \in N_m$  (binary).

$R_{mnl}$  equal to 1 iff in node  $n \in N$  a receiving transponder on wavelength  $l \in L$  is used to receive a signal from node  $m | n \in N_m$  (binary).

#### 4.1.2 Objective function

$$\text{minimise} \left\{ \Pi_e \sum_r \sum_{i \neq s(r)} \sum_{j \neq i} X_{ij}^r * t_r + \Pi_t \sum_l \sum_{(m,n)} [T_{mnl} + R_{mnl}] + \frac{\Pi_o}{C} \sum_l \sum_i \sum_{j \neq i} [V_{ijl} + \sum_{(m,n)} P_{mnl}^{ij}] \right\}$$

In the first term, for each request, we compute the total number of intermediate nodes where electronic processing is accomplished. The second term accounts for the total power consumed in every physical link over all wavelengths by transmitting and receiving transponders. Finally, the third term computes the total optical switching power contribution. Note that this contribution depends on the time during which SOAs are active. Indeed, the ratio between this time period and the total observation time is proportional to the ratio between the bandwidth of an SVP and the total capacity  $C$  of a wavelength. Therefore for each lightpath (i.e. for each couple of nodes  $(i, j)$  and for each wavelength  $l$ ), we weight the total traffic switched in the nodes  $[V_{ijl} + \sum_{(m,n)} P_{mnl}^{ij}]$  by the total capacity  $C$ . Then,

this result is multiplied by  $\Pi_o$  to obtain the final optical switching contribution.

### 4.1.3 Subject to

$$\sum_{j \neq i} X_{ij}^r - \sum_{j \neq i} X_{ji}^r = \begin{cases} 1, & \text{if } i = s(r) \\ -1, & \text{if } i = d(r) \\ 0, & \text{otherwise} \end{cases} \quad \forall i \in N, \forall r \in R \quad (2)$$

$$\sum_l Y_{ijl}^r = X_{ij}^r * t_r \quad \forall i, j \in N | i \neq j, \forall r \in R \quad (3)$$

$$\sum_r Y_{ijl}^r = V_{ijl} \quad \forall i, j \in N | i \neq j, \forall l \in L \quad (4)$$

$$\sum_{n \in N_m} P_{mnl}^{ij} - \sum_{n | m \in N_n} P_{mnl}^{ij} = \begin{cases} V_{ijl}, & \text{if } m = i \\ -V_{ijl}, & \text{if } m = j \\ 0, & \text{otherwise} \end{cases} \quad \forall m, i, j \in N | i \neq j, \forall l \in L \quad (5)$$

$$\sum_i \sum_{j \neq i} P_{mnl}^{ij} \leq C \quad \forall (m, n) \in A, \forall l \in L \quad (6)$$

$$T_{mnl} \geq \frac{1}{C} \sum_{j \neq m} P_{mnl}^{mj}, \quad R_{mnl} \geq \frac{1}{C} \sum_{i \neq n} P_{mnl}^{in} \quad \forall (m, n) \in A, \forall l \in L \quad (7)$$

Equations (2) impose the continuity of flow at the logical (IP) layer (solenoidality constraint) and also force the requests to be served by lightpaths over the same logical paths (traffic is not bifurcated at the logical layer). (3) state that, for each request, the amount of traffic between each logical link to be carried by each wavelength is equal to  $Y_{ijl}^r$ . The total amount of traffic carried by each wavelength between the logical links is computed by (4). (5) impose the solenoidality constraint at the physical layer, where, unlike the logical layer, traffic-bifurcation is allowed. The capacity constraint is formulated by constraints (6), where every wavelength in each physical link is forced not to carry an amount of traffic higher than the wavelength capacity. Finally, constraints (7) compute the number of transmitting and receiving transponders used in each node over each  $\lambda$ . Compared with traditional architectures where each transponder can support traffic towards a single destination, in a TDS network a single transmitter sends its traffic towards different destinations, provided that the intermediate switches get reconfigured and switch the signal over different paths. So these two set of constraints represent the main novelty compared to existing double-layer network flow problem and, in other words, the capability of TDS to perform grooming in the optical layer is represented by this property captured by these constraints.

### 4.2 On the physical impairment constraint

When optical signals traverse different network elements (fibre links, EDFAs, OXCs etc.) without being converted into the electronic domain (i.e. without being ‘regenerated’) their quality, in terms of optical signal-to-noise ratio (OSNR), can be substantially reduced. So far, we have not included in the ILP formulation any limitations neither on the physical length of the links nor on the number of OXCs traversed by the optical signal. If the penalty introduced

by these factors exceeds a given threshold, OE and EO conversion are needed to regenerate the optical signal in the electronic domain. Signal regeneration is accomplished whenever electronic processing is performed at the IP layer, so we need to introduce an additional constraint to the formulation (2)–(7), so that optical signals are forced to be transferred into the electronic domain and regenerated, when necessary. To evaluate the limitations on the distance that can be covered without performing regeneration (i.e. transparent reach) we refer to the model described in [17]. The minimum value of the  $Q$  factor, when no error correction at the receiver is performed, is 17 dB. Assuming a conservative margin of 3 dB that accounts for the non-linear effects, the constraint over the  $Q$  factor can be expressed in terms of the  $OSNR_{e2e}$ , that is, the optical end-to-end (e2e) signal-to-noise ratio (in dB) at the receiver node of the logical link (i.e. of a transparent path), imposing  $OSNR_{e2e} \geq 20$  dB. The  $OSNR_{e2e}$  depends on the distance and the number of nodes traversed by the optical signal and is computed as follows

$$OSNR_{e2e} = 10 \log_{10}(\rho_{total}), \quad \text{where } \frac{1}{\rho_{total}} = \sum_i \frac{1}{\rho_i} \quad (8)$$

$\rho_i$  is the OSNR in linear units of the generic  $i$ th component (link or OXC) of the transparent path, that is,  $\rho_i = 10^{OSNR_i/10}$ , and is calculated assuming maximum span length of 85 km and noise figures values for the different components (amplifiers, OXCs etc.) as in [17]. By doing so, we are able to evaluate  $\rho_i$  for each physical link (i.e.  $\rho_{mn}$  with  $(m, n) \in A$ ) and for each node of the network (i.e.  $\rho_n$  with  $n \in N$ ) [The values of  $\rho_n$  do not depend on the characteristics of the links, but only on the technology used in the node, that is, the kind of considered OXC. Therefore we assume  $\rho_n = \rho_{node} = \text{constant} \cdot \forall n \in N$ ]. Referring to [17], the value of  $\rho_{node}$  decreases proportionally to the switching fabric attenuation increase. In TDS architectures we assume that switches have a limited number of ports (we use several switch-planes operating at the proper wavelength). Therefore according to (1), we have at least a 1 dB input-to-output gain for the SOA-based switches, that leads to a much higher  $OSNR_{node}$  in TDS switches if compared to those considered in [17] (about two orders of magnitude in linear units), where the input-to-output attenuation of the switch matrix is 12 dB. Moreover, note that the value of  $\rho_{node}$  is much higher than the various  $\rho_{mn}$ , that is, the effect over the physical impairments produced by the nodes is negligible if compared with the links, almost independently on the OXC-technology.

Assuming  $H$  is the number of OXCs traversed by an optical signal, we have

$$OSNR_{e2e} = -10 \log_{10} \left( \frac{H}{\rho_{node}} + \sum_{(m,n)} \frac{1}{\rho_{mn}} \right) \Rightarrow \frac{H}{\rho_{node}} + \sum_{(m,n)} \frac{1}{\rho_{mn}} \leq 10^{-2} \quad (9)$$

where the sum is performed over all the links  $(m, n) \in A$  belonging to the considered logical link. To express this constraint within the ILP formulation of Section 4.1 we need to define two additional binary variables, that is:



$v_{ijl}$  ‘binarisation’ of variable  $V_{ijl}$ , that is, it is equal to 1 iff  $V_{ijl} > 0$ .

$Q_{mnl}^{ij}$  ‘binarisation’ of variable  $P_{mnl}^{ij}$ , that is, it is equal to 1 iff  $P_{mnl}^{ij} > 0$ .

More formally, these two variables are obtained by imposing the two following sets of constraints

$$v_{ijl} \leq V_{ijl}, \quad B * v_{ijl} \geq V_{ijl} \quad \forall i, j \in N | i \neq j, \forall l \in L \quad (10)$$

$$Q_{mnl}^{ij} \leq P_{mnl}^{ij}, \quad B * Q_{mnl}^{ij} \geq P_{mnl}^{ij} \quad \forall (m, n) \in A, \quad \forall i, j \in N | i \neq j, \forall l \in L \quad (11)$$

where  $B$  is a ‘big’ number (i.e.  $B = 10^9$ ) used to ‘binarize’ the integer variables. Thus we account for the physical impairment constraint (9) imposing the following set of linear inequalities

$$\frac{1}{\rho_{\text{node}} \sum_{(m,n)} [Q_{mnl}^{ij} + v_{ijl}]} + \sum_{(m,n)} \frac{Q_{mnl}^{ij}}{\rho_{mn}} \leq 10^{-2} \quad \forall i, j \in N | i \neq j, \forall l \in L \quad (12)$$

Although optical signal regeneration is here considered to be performed by IP routers, in order to achieve energy consumption reduction we can also consider 3R-regenerators, which allow us to perform signal regeneration directly at the optical layer (typically referred as translucent

optical network design [18]). Their placement in TDS networks is still an open issue since the introduction of time-dimension implies an additional degree of freedom. For example, the problem of regenerators placement in a classical IPoWDM network neglects the fact that the same resource (i.e. the same regenerator) can be employed to regenerate more than one optical signal that traverse it in different TFs. Therefore such a problem, combined with a preliminary energy-and-regenerators aware scheduling session of the different connection requests, can help to save large amount of energy within TDS transport networks.

### 5 Case-studies and results

The ILP formulation of the previous section has been studied over two different network topologies and results obtained for the TDS case have been compared to a classical IPoWDM architecture (T. IP-BG described in [3]), where the effect of physical impairments is also considered. In the IPoWDM architecture, optical bypass is implemented and grooming/degrooming operations are performed when necessary in IP-routers. Moreover, when signal regeneration is required, the signal needs to be transferred into the electronic domain, as for the TDS case. In Figs. 5a and b we show the IPoWDM and TDS architectures, respectively, considered for the comparison as well as the establishment of three connection requests (continuous arrows) over different lightpaths (dashed arrows). For both architectures, signal regeneration is accomplished in the IP-router (left node). Add/drop operations, performed for both architectures in the right

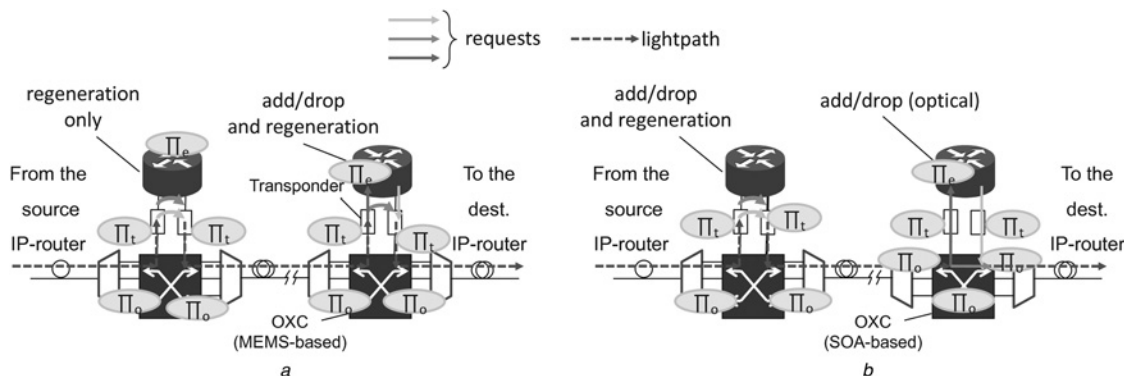


Fig. 5 Compared architectures

- a IPoWDM: traffic grooming is accomplished by terminating lightpaths and performing electronic processing
- b TDS: traffic grooming is accomplished in the electronic domain through the establishment of SVPs

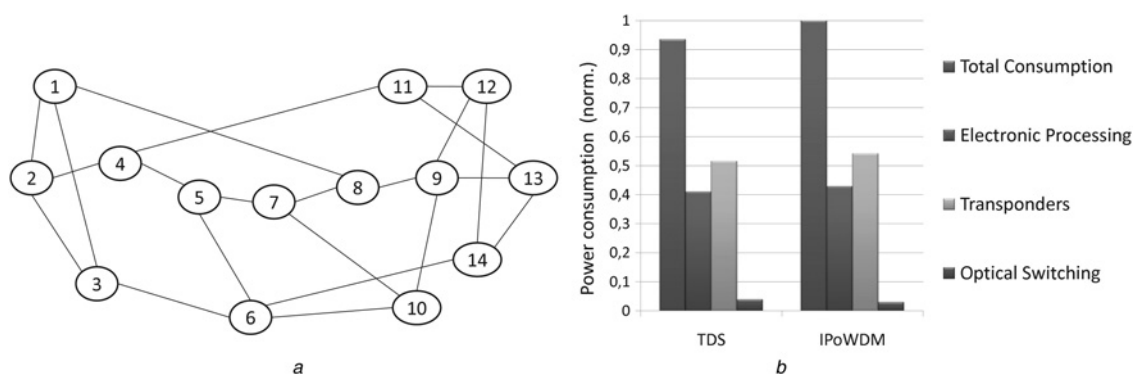


Fig. 6 Case study and results

- a NSFNET network topology
- b Total power consumption comparison and different contributions

node, are differently accomplished. Unlike the TDS case, where grooming can be performed directly in the optical domain, in the IPoWDM case signal add/drop is accomplished by terminating the established lightpath and performing grooming in the IP router, thus electronic processing is needed. In this figure we also show the different power contributions needed in the two cases to establish the three requests.

A non-uniform traffic matrix with a total amount of traffic of 180 Gbit/s as in [19] has been considered for the NSFNET network topology, shown in Fig. 6a and consisting of 14 nodes and 22 bidirectional links [we have considered this topology as it is a well-studied reference topology in the literature. For networks with higher number of nodes, obtaining optimal solutions is harder, because of the problem-complexity. Thus heuristics/simulations could be considered to carry out the power consumption evaluation, but this issue is out of the purpose of this paper and will be addressed in a future work]. We have considered mono-fibre network links with  $W = 11$  wavelengths per fibre [this is the minimum number of wavelengths that guarantees the feasibility of the solution for both the architectures], where each wavelength has capacity  $C = 10$  Gbit/s. The values of  $\rho_{mn}$  and  $\rho_{node}$  are computed as explained in the previous section. We have used CPLEX 12.0 solver on a workstation equipped with  $8 \times 2.00$  GHz processors and with 32 GByte of RAM.

In Fig. 6b the obtained total power consumption and the different contributions (normalised to the maximum value) are shown for the two architectures. The consumption of the TDS architecture is lower than the IPoWDM case. As we expected, this is because of the fact that in TDS architecture, traffic grooming can be performed in the optical domain, with no need for the signals to be converted into the electronic domain and processed by IP routers to perform electronic grooming. This results in the reduction of the amount of electronic processing needed and especially of the number of transponders used, and therefore implies lower consumption in the TDS architecture if compared to the IPoWDM case. Power consumption values have also been compared by considering an increasing value of the total required bandwidth, that is, the bandwidth required by each connection has been scaled by a factor of 2, 3, 4 and 5 [for these cases, the number of wavelengths per fibre  $W$  has been correspondingly increased to 15, 23, 30 and 37 wavelengths per fibre]. The first set of results in Table 1 shows the comparison between the IPoWDM and TDS total power consumption, when we impose to both architectures the physical impairment constraint of (12), that is,  $OSNR_{e2e} \geq 20$  dB. The results are shown for the different scaling factors (1, 2, 3, 4 and 5 shown in the first column of Table 1). We observe that TDS power consumption is maintained always below the consumption of the IPoWDM

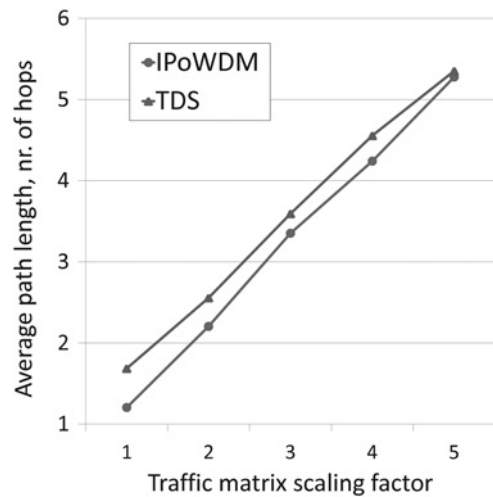


Fig. 7 Average path length in the TDS case for increasing total required traffic

architecture and for increasing traffic amounts the gap between the two architectures remains nearly unchanged, mainly because of the limitation imposed by the physical impairment constraint (12), that implies higher amount of electronic processing and transponders needed. Similar results are also obtained for the COST239 network topology shown in [20], but we do not shown them here for sake of conciseness.

The energy-advantage of the TDS case is obtained at the cost of longer routes, as can be observed in Fig. 7, where we show the average number of links traversed by connection requests from source to destination. This may result in higher delays experienced by signals in TDS networks, thus representing a drawback of such architectures. Note that this difference decreases as traffic-granularity increases, since the number of grooming operations performed in the IPoWDM case is lower, so the average path-length of connection requests in IPoWDM networks approaches that of the TDS case. Thus, for increasing traffic, the delay drawback of TDS networks is reduced.

For different values of the total required bandwidth, we have also investigated the power consumption of the two architectures relaxing constraints (12). Specifically, we impose the  $OSNR_{e2e}$  value assumes, for each end-to-end transparent path, a minimum value of 19, 18 and 17 dB, and the results are shown in Table 1 as well. We note that, progressively relaxing the constraint over the minimum end-to-end OSNR, the gap in the power consumption between the two architectures gradually increases. At higher traffic loads the gap can be observed even for a slight relaxation of the constraint over the end-to-end OSNR (i.e.  $OSNR_{e2e} \geq 19$  dB) whereas, as the constraint is further relaxed, the gap between IPoWDM and TDS architectures

Table 1 Power consumption values (in kW) for the two architectures with varying scaling factor and  $OSNR_{e2e}$  threshold

Traffic matrix scaling factor	$OSNR_{e2e} \geq 20$ dB		$OSNR_{e2e} \geq 19$ dB		$OSNR_{e2e} \geq 18$ dB		$OSNR_{e2e} \geq 17$ dB	
	IPoWDM	TDS	IPoWDM	TDS	IPoWDM	TDS	IPoWDM	TDS
1	5.478	5.122	4.107	3.688	3.585	2.114	3.135	1.357
2	10.479	9.957	7.273	6.098	5.813	3.953	4.596	2.661
3	15.372	14.805	10.163	8.647	8.112	5.325	6.176	3.82
4	20.194	19.466	13.258	10.3	10.185	7.09	7.489	5.097
5	24.867	24.224	15.78	12.178	11.981	8.7	8.377	6.24



**Table 2** Percentage of power savings obtained in the TDS case for varying scaling factor and OSNR<sub>e2e</sub> threshold

Traffic matrix scaling factor	OSNR <sub>e2e</sub> ≥ 20 dB, %		OSNR <sub>e2e</sub> ≥ 19 dB, %		OSNR <sub>e2e</sub> ≥ 18 dB, %		OSNR <sub>e2e</sub> ≥ 17 dB, %	
	α = 10	α = 20	α = 10	α = 20	α = 10	α = 20	α = 10	α = 20
	1	6.47	5.76	26.06	26.74	48.31	49.58	58.78
2	1.07	1.35	13.23	15.81	38.32	40.18	44.78	44.45
3	3.9	4.37	15.14	16.64	34.73	35.69	38.42	38.74
4	3.81	3.55	9.61	11.99	30.66	30.93	32.31	32.69
5	2.79	2.78	9.79	10.51	26.49	33.82	24.35	25.37

significantly increases also for lower traffic loads, until the case of OSNR<sub>e2e</sub> ≥ 17 dB, in which TDS provides more than 55% of power savings with respect to the IPoWDM architecture. In this case electronic processing is mainly needed to perform grooming of traffic (rather than signal regeneration), thus the capability in performing traffic grooming directly in the optical domain makes the TDS even more energy-efficient than the IPoWDM architecture. We also note that, especially for higher traffic loads, imposing more stringent physical impairment constraint (i.e. moving from the right to the left in Table 1), produces a higher step in TDS consumption if compared to the IPoWDM one. This means that, if the receivers technology accepts optical signals with minimum OSNR<sub>e2e</sub> equal to 19 dB (or less), substantial increase in the TDS energy-efficiency will be obtained, even for lower traffic loads.

A further comparison between the two architectures has been carried out considering a power consumption improvement envisioned in routers technology for the near future. Specifically, we have considered that the values of  $\Pi_e$  and  $\Pi_t$  described in Section 3 are reduced by a factor  $\alpha = 10\%$  and  $\alpha = 20\%$ , respectively. The results obtained in these two cases are drawn in Table 2, where we show the percentage of power savings obtained with the TDS architecture for different traffic scenarios and for different values of the OSNR<sub>e2e</sub> threshold. Also in these cases we observe that the TDS architecture outperforms the IPoWDM one, especially for lower bandwidth granularity and for less strict physical impairment constraint, when we can obtain up to about 60% of power saving.

The main findings obtained in this paper can be resumed as follows: (i) TDS architecture provides power savings if compared to the IPoWDM architecture, thanks to the reduction of the number of transponder used and the amount of electronic traffic processing performed; (ii) when strict physical layer impairment constraints are considered, the difference among the power consumption of the two architectures is substantially reduced. However, as these constraints are relaxed (i.e. assuming better receivers technology), the TDS energy efficiency increases and in some cases power savings higher than 55% can be reached; (iii) the TDS against IPoWDM behaviour is also maintained when a global improvement factor of 10 or 20% is considered for IP routers power consumption (electronic processing and transponders contributions), so that power savings of about 60% can be reached with TDS.

## 6 Conclusions

In this paper we have investigated the power consumption of a recently proposed transport technique, known as time-driven switching (TDS), that enables to perform traffic grooming in the wavelengths bandwidth directly in the optical domain. We have demonstrated that significant power savings, up to 55%

or more, can be obtained with respect to a classical IP over WDM architecture, which make TDS-based optical networks a promising candidate to cope with the envisioned high growth the Internet will face within the next 10 years. A physical-impairment-aware ILP formulation has been developed to evaluate the power consumption of the different transport architectures. In a future work we will investigate the possibility of performing regeneration of signals directly in the optical domain. The impact over the energy consumption of the whole transport network, produced by the architecture of the considered SOA-based optical switches has also been studied.

## 7 Acknowledgments

The research leading to these results has received funding from the European Union Seventh Framework Programme (FP7/2007-2013) under grant agreement no. 257740 (Network of Excellence 'TREND') and from the Italian Ministry of Education under PRIN 2008 grants for the project 'BESOS' (Bandwidth efficiency and Energy Saving by sub-lambda Optical Switching).

## 8 References

- 1 Yetginer, E., Rouskas, G.: 'Power efficient traffic grooming in optical WDM networks'. Proc. IEEE Global Telecommunications Conf. (GLOBECOM), Honolulu, HI-USA, November 2009, pp. 1–6
- 2 Shen, G., Tucker, R.S.: 'Energy-minimized design for IP over WDM networks', *IEEE/OSA J. Opt. Commun. Netw.*, 2009, 1, (1), pp. 176–186
- 3 Musumeci, F., Vismara, F., Grkovic, V., Tornatore, M., Pattavina, A.: 'On the energy efficiency of optical transport with time driven switching'. Proc. Int. Conf. on Communications (ICC), Kyoto, Japan, June 2011, pp. 1–5
- 4 Baldi, M., Ofek, Y.: 'Fractional lambda switching – principles of operation and performance issues', *SIMULATION: Trans. Soc. Mode. Simul. Int.*, 2004, 80, (10), pp. 527–544
- 5 Gallep, C., Conforti, E.: 'Reduction of semiconductor optical amplifier switching times by prepulse step-injected current technique', *IEEE Photonics Technol. Lett.*, 2002, 14, (7), pp. 902–904
- 6 Pattavina, A.: 'Switching theory. Architectures and performance in broadband ATM networks' (John Wiley & Sons, 1998, 1st edn.)
- 7 'COM-1300 PCMCIA/CardBus FPGA DEVELOPMENT PLATFORM'. <http://comblock.com/download/com1300.pdf>, accessed October 2011
- 8 'Xilinx power estimator'. <http://www.xilinx.com>, accessed October 2011
- 9 'LEA-6 u-blox 6 GPS modules data sheet'. <http://www.u-blox.com/>, accessed October 2011
- 10 'Cisco CRS-1 carrier routing system 16-slot line card chassis specifications'. <http://www.cisco.com>, accessed October 2010
- 11 'Cisco 40-channel single-module ROADMs'. <http://www.cisco.com>, accessed October 2010
- 12 Connelly, M.: 'Wideband semiconductor optical amplifier steady-state numerical model', *IEEE J. Quantum Electron.*, 2001, 37, (3), pp. 439–447
- 13 Agrawal, D., Baldi, M., Corrà, M., et al.: 'Scalable switching testbed not "Stopping" the serial bit stream'. Proc. IEEE Int. Conf. on Communications (ICC), Glasgow, Scotland, June 2007, pp. 2269–2274
- 14 Yu, J., Jeppesen, P.: 'Improvement of cascaded semiconductor optical amplifier gates by using holding light injection', *IEEE/OSA J. Lightwave Technol.*, 2001, 19, (5), pp. 614–623

- 15 Yang, Q., Kelley, K.: 'Effect of backward ASE noise on the gain distribution in a cascade of SOA switches'. Digest of the LEOS Summer Topical Meetings on Biophotonics/Optical Interconnects and VLSI Photonics/WBM Microcavities, San Diego, CA-USA, June 2004, pp. 57–58
- 16 Koyama, F., Uenohara, H.: 'Noise suppression and optical ASE modulation in saturated semiconductor optical amplifiers'. Proc. Asilomar Conf. on Signals, Systems and Computers, Pacific Grove, CA-USA, November 2004, pp. 98–102
- 17 Yannuzzi, M., Quagliotti, M., Maier, G., *et al.*: 'Performance of translucent optical networks under dynamic traffic and uncertain physical-layer information'. Proc. IEEE Int. Conf. on Optical Network Design and Modeling (ONDM), Braunschweig, Germany, February 2009, pp. 1–6
- 18 Ramamurthy, B., Feng, H., Datta, D., Heritage, J.P., Mukherjee, B.: 'Transparent vs. opaque vs. translucent wavelength-routed optical networks'. Proc. on Optical Fiber Communication, National Fiber Optic Engineers Conf. (OFC/NFOEC), San Diego, CA-USA, February 1999, pp. 59–61
- 19 Miyao, Y., Saito, H.: 'Optimal design and evaluation of survivable WDM transport networks', *IEEE J. Sel. Areas Commun.*, 1998, **16**, (7), pp. 1190–1198
- 20 Liu, M., Tornatore, M., Mukherjee, B.: 'New and improved strategies for optical protection in mixed-line-rate WDM networks'. Proc. Conf. on Optical Fiber Communication, National Fiber Optic Engineers Conf. (OFC/NFOEC), San Diego, CA-USA, March 2010, pp. 1–3